Available online at www.sciencedirect.com
ScienceDirect
International Journal of Heat and Mass Transfer 50 (2007) 2139–2147
International Journal of HEAT and MASS TRANSFER
www.elsevier.com/locate/ijhmt

Numerical investigation on enhancement of oxygen transfer by forced convection in liquid lead–bismuth eutectic system

Yitung Chen [a], Huajun Chen [a,*], Jinsuo Zhang [b]

[a] *Department of Mechanical Engineering, University of Nevada Las Vegas, NV 98154, USA*
[b] *International Nuclear System Engineering Group, Los Alamos National Laboratory, NM 87545, USA*

Received 30 September 2005; received in revised form 4 October 2006
Available online 16 January 2007

Abstract

Lead–bismuth eutectic (LBE) technology is being developed as a primary candidate for a nuclear coolant in accelerator-driven systems and advanced reactors. However, the corrosion of containment and structural materials remains a major issue. Properly controlling the low oxygen level in LBE to mitigate corrosion proves effective under certain conditions. To mix the oxygen uniformly and quickly, the forced convection is proposed to enhance the oxygen transport with using cover gas scheme. A lattice Boltzmman simulation of LBE flow and oxygen transport in a simplified container was carried out to explore characteristics of the oxygen transport. The oxygen control technique with cover gas scheme is formulated. To find more efficiency way to mix the oxygen, three different forced convection flow patterns on the oxygen transport are investigated. The simulation results show that the force convections induced by all the boundary conditions greatly enhance the oxygen transport in the liquid metal of our system. Both of transient oxygen distribution, oxygen diffusion time, and average Sherwood number at the interface are investigated and some useful information are also provided to calibrate low concentration level oxygen sensors.

Keywords: Oxygen transfer; Forced convection; Lattice Boltzmann method; Lead–bismuth eutectic

1. Introduction

Recently, lead bismuth eutectic (LBE) technology is being developed for applications in advanced nuclear systems and high power spallation neutron target. However, corrosion of containment and structural materials presents a critical challenge in the use of liquid lead or lead–bismuth eutectic (LBE). One of the approaches to reduce the corrosion is controlling the oxygen concentration for forming a protective oxide film on the structure surfaces. Such technique was first developed and deployed in Russia [1–3], and then extensively studied worldwide [4,5]. The ongoing R&D activities devoted to oxygen control technique consist of sensor and control system development, and corrosion tests. The active oxygen control technique exploits the fact that lead and bismuth are chemically less active than the major components of steels, such as Fe, Ni, and Cr. By carefully controlling the oxygen concentration in LBE, it is possible to maintain an iron and chrome based oxide film on the surfaces of structural steels, while keeping lead and bismuth from excessive oxidization that can lead to precipitation contamination. The oxide film effectively separates the substrates from LBE. Once this oxide film is formed on the structure surface, the direct dissolution of the structural materials becomes negligible because the diffusion rates of the alloying components are very small in the oxides [6].

For controlling the oxygen level in the liquid metals, several oxygen control systems have been developed, including injection of hydrogen and steam mixture and cover gas

---

[*] Corresponding author. Address: Department of Mechanical Engineering, University of Nevada Las Vegas, 4505 Maryland Parkway, Box 454027, Las Vegas, NV 89154-4027, USA. Tel.: +1 702 895 2338; fax: +1 702 895 3936.
E-mail address: huajunc@nscee.edu (H. Chen).

0017-9310/$ - see front matter © 2006 Elsevier Ltd. All rights reserved.
doi:10.1016/j.ijheatmasstransfer.2006.11.002

Nomenclature

a_{Pb}	activity of lead
C	oxygen concentration
D	diffusion coefficient of oxygen in LBE (m^2/s)
$\mathbf{e}$	dimensionless lattice discrete velocity
f	distribution function of liquid metal
g	distribution function of the concentration of oxygen
L	width of the square container
K	mass transfer coefficient (m/s)
n	normal direction of the wall
P_{O_2}	oxygen partial pressure (atm)
P_{H_2O}	water vapour partial pressure (atm)
P_{H_2}	hydrogen partial pressure (atm)
R	gas constant
Re	Reynolds number, $Re = \rho U_0 L/\mu$
Sc	Schmidt number, $Sc = \upsilon/D$
Sh	Sherwood number, $Sh = KL/D$
t	time (s)
T	temperature (K)
$\mathbf{u}$	velocity (m/s)
U_0	inlet velocity (m/s)
$\mathbf{x}$	position vector
x, y	coordinates

Greek symbols

ρ	density (kg/m^3)
μ	dynamic viscosity (kg/m/s)
υ	kinematic viscosity (m^2/s)
ω_i	weight coefficients
τ	relaxation time
Δx	spacing of a lattice
$\Delta G_{Fe_3O_4}$	standard free energy of formation of Fe_3O_4 (J/mol)
ΔG_{PbO}	standard free energy of formation of PbO (J/mol)

Subscripts

eq	equilibrium
w	wall
0	reference value
b	bulk

systems [2]. When depletion or excess of oxygen in the liquid metals is detected by oxygen sensors, the most straightforward method for adjusting the oxygen level is to inject oxygen or hydrogen with inert carrier gases such as helium or argon. Considering the efficient reactions between the injected oxygen and liquid lead, this method may lead to heavy slag formation that can be transferred and settled in various areas and may lead to flow blockage or system failure.

Another cover gas system is based on certain equilibrium reaction systems, e.g. a hydrogen and steam mixture [5,7]. The targeted oxygen level can be achieved by controlling the ratio of the partial pressures of hydrogen and steam if the reaction is at sufficiently high temperature and can reach equilibrium. This method can achieve very low stable oxygen level compared with the direct injection of oxygen/hydrogen. However, since the kinetics of oxygen transfer in the system with cover gas scheme is controlled by the diffusion process, it is not very effective and oxygen transfer rate is very slow currently for large adjustment. Therefore, mixing oxygen of such a low concentration in LBE system in a uniform and quick way becomes more and more important.

Meanwhile, a stable, uniform and extremely low oxygen concentration in the liquid lead or LBE is also the first requirement for calibrating the oxygen sensor. Measuring oxygen concentration in high temperature liquid lead or LBE can be achieved reliably with the solid electrolyte sensors [8]. A zirconia-based solid electrolyte sensor for the oxygen-concentration measurement in LBE has been developed by Darling and Li [9]. However, the characteristics of this sensor have not been well examined. One application of our current study is to design a well-controlled system for calibrating and testing the sensor.

Hence, in order to uniformly and quickly mix oxygen in LBE system, we propose a new method of using forced convection to enhance the oxygen transfer in liquid metals instead of pure diffusion by cover gas scheme. To guide our design for new mixing apparatus, we first numerically simulate oxygen-mixing processes in a 2-D rectangular container under different operating conditions to study the forced convection mixing characteristics and estimate the time for concentration equilibrium. In our simulation, the forced convection metal flow as well as mass transfer are simulated by lattice Boltzmann method, which has been successfully applied to study a variety of flow and transport phenomena such as in multi-component flows [10–12], multiphase flow [13], turbulence [14,15], and porous media [16].

In the present paper, three different inlet–outlet boundary conditions are applied for creating natural convection mixing. Oxygen is introduced from the top of the container by using cover-gas scheme, and the free surface boundary condition is used at the interface between the gas and the liquid metal. A static free surface is assumed for the laminar liquid metal flow. The local and average Sherwood numbers at the interface are examined to predict the oxygen transfer rate into the liquid metal for different Reno numbers (*Ra*) and Schmidt numbers (*Sc*). Finally, the critical time to reach the uniform oxygen concentration is determined for each temperature boundary condition.

2. Oxygen control technique with cover gas scheme

The purpose of oxygen control in a liquid lead-alloy system is not only to form and maintain the protective layers, but also to prevent lead oxide precipitation, which would lead to plugging of the loop. The oxygen concentration should be controlled in a proper range. As indicated in Ref. [8], the oxygen partial pressure in the gas phase must be higher than that required for oxidation of iron, the main steel component, and lower than that for PbO formation. Hence, the initial oxygen partial pressure should be controlled in

$$\exp\left(\frac{\Delta G_{\mathrm{Fe_3O_4}}}{2RT}\right) \leqslant P_{\mathrm{O_2}} < \frac{1}{a_{\mathrm{Pb}}^2}\exp\left(\frac{2\Delta G_{\mathrm{PbO}}}{RT}\right) \tag{1}$$

where $P_{\mathrm{O_2}}$ are the oxygen partial pressure, a_{Pb} is the activity of Pb, R is the gas constant, T is the temperature, $\Delta G_{\mathrm{Fe_3O_4}}$ and ΔG_{PbO} are the standard free energy of formation of Fe_3O_4 and PbO, respectively. For non-isothermal LBE systems (350–550 °C):

$$1.01\times10^{-27} \leqslant P_{\mathrm{O_2}}\ (\mathrm{atm}) < 4.29\times10^{-26} \tag{2}$$

There are several ways to control the oxygen level. One of them is to control the oxygen partial pressure in the cover gas system. Since the required oxygen level is very low, it is not possible to use an oxygen/inert gas mixture, e.g. O_2/Ar, to directly control the oxygen concentration in the liquid metal. Therefore, a mixture of argon, hydrogen and vapor is often used to cover the liquid LBE. This chemical reaction systems is also particular attractive since hydrogen can be used to reduce PbO contaminant as well. The relation between the partial pressure and the ratio of hydrogen and water vapor is given by

$$P_{\mathrm{O_2}} = \left(\frac{P_{\mathrm{H_2O}}}{P_{\mathrm{H_2}}}\right)^2 \exp\left(\frac{2\Delta G_{\mathrm{H_2O}}}{RT}\right) \tag{3}$$

From the above equation, it is evident then that the ratio of hydrogen and water vapor determines the partial pressure of oxygen. Once we know the oxygen partial pressure, it is easy to get the oxygen concentration by the relation between oxygen concentration and partial pressure [8].

In the interface of gas/liquid phase, the oxygen transport is controlled by equilibration between gas phase and liquid metal in the reaction container. The kinetic process of oxygen transport, which determines the timescale of oxygen control process by cover gas scheme, is diffusion. The exchange of oxygen atoms through the interface between the gas phase and the liquid metal can be modeled by the diffusion equations

$$\partial C/\partial t = D\nabla^2 C \tag{4}$$

where C is the oxygen concentration in LBE and D is the oxygen diffusion coefficient in LBE. By using of Laplace transformation, a time-dependent solution for oxygen uptake or loss with a constant diffusion coefficient results can be obtained if a rigid plane of stagnant liquid metal and the constant oxygen concentration on the surface are assumed [7],

$$C_{\mathrm{bulk}}/C_\infty = 1 - \sum_{n=0}^{\infty}\frac{8}{(2n-1)^2\pi^2}\exp\left(-\frac{D(2n+1)^2\pi^2 t}{4h^2}\right) \tag{5}$$

where C_{bulk} is the bulk oxygen concentration in liquid metal at a time t and h is the height of liquid metal container.

According to the estimate of Zhang and Li [6] by using Stokes–Einstein equation, the oxygen diffusion coefficient in the liquid lead or LBE, D, is $\sim10^{-8}\ \mathrm{m^2/s}$ at 500 °C. If we take $D = 1\times10^{-8}\ \mathrm{m^2/s}$ and $h = 0.2$ m, the time for $C_{\mathrm{bulk}}/C_\infty$ to reach 90% is $\sim10^6$ s according to Eq. (5). Since it takes a long tome to transfer the oxygen to the wall by pure diffusion, the oxide layer can not formed at the initial stage and the severe corrosion behavior will be found. Hence, to mitigate the corrosion at the initial stage and transport the oxygen into LBE quickly, we propose to use forced convection to enhance the mixing of oxygen transfer, as seen in Fig. 1. Here, to find a best mixing mode, three kinds of different force convection mode for our experimental setup of containers in nuclear engineering applications are considered. The widths of inlet and outlet are taken as $L/32$. It is assumed that the dissolving oxygen concentration at the liquid surface is a constant and the oxygen in LBE flow after pass through outlet is well mixed. At the inlet, the velocity distribution of the liquid LBE flow is taken as uniform and the oxygen concentration has the same value as the average value at the outlet.

3. Lattice Boltzmann model for oxygen transport

In this work, it is assumed that the oxygen concentrations are sufficiently low not to influence to the LBE flow. The two-dimensional nine-velocity model is used in this work, where the physical space is divided into square lattices. In this section, the following non-dimensional variables are used as the same as that in Ref. [12]. The oxygen transport in such a system can be described by the following lattice Boltzmann equation

$$g_i(\mathbf{x}+\mathbf{e}_i\Delta x, t+\Delta t) - g_i(\mathbf{x},t) = -\frac{g_i(\mathbf{x},t)-g_{i,\mathrm{eq}}(\mathbf{x},t)}{\tau}\qquad i=0,\ldots,8 \tag{6}$$

where g_i is the distribution function of the concentration of iron or oxygen; τ is the relaxation time; Δx is the spacing of square lattice; Δt is a time step during which the particle travel the lattice spacing; $\mathbf{e}_i$'s are the discrete velocity, for 2D nine-speed LBM model, we have

$$\mathbf{e_i} = \begin{cases} 0, \quad i=0 \\ (\cos[\pi(i-1)/2], \sin[\pi(i-1)/2]) \\ \quad i=1,\ldots,4 \\ \sqrt{2}(\cos[\pi(i-5)/2+\pi/4], \sin[\pi(i-5)/2]+\pi/4) \\ \quad i=5,\ldots,8 \end{cases} \tag{7}$$

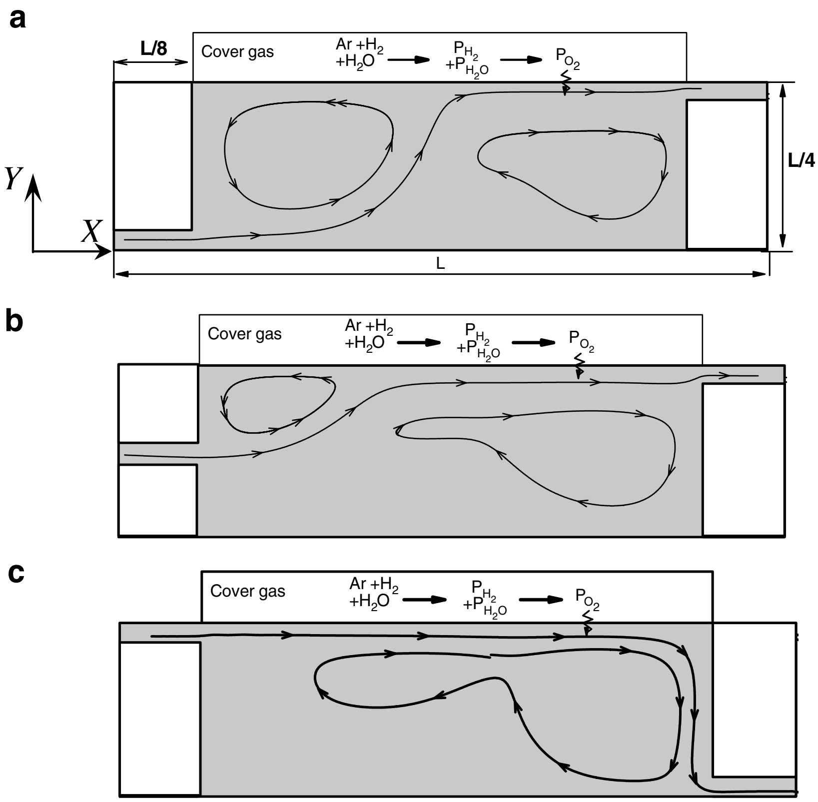

Fig. 1. Schematic of the simplified geometry for our container. Three different schemes for the inlet and outlet are considered: (a) the inlet locates near bottom and outlet locates at the top, (b) the inlet locates at the middle height bottom and outlet locates at the top and (c) the inlet locates at the top and outlet locates at the bottom. The width of the inlet and outlet is $L/32$. Oxygen input is from the cover gases at the top of the container.

$g_{i,\mathrm{eq}}$ is the corresponding equilibrium distribution:

$$g_{i,\mathrm{eq}} = \omega_i C(1 + 3\mathbf{e}_i \cdot \mathbf{u}) \tag{8}$$

where C is the concentration of oxygen and ω_i's is the weight coefficients, $\omega_0 = 4/9$, $\omega_i = 1/9$ for $i = 1, \ldots, 4$, $\omega_i = 1/36$ for $i = 5, \ldots, 8$. The concentrations of oxygen and iron can be calculated by

$$C = \sum_i g_i \tag{9}$$

The evolution of particle distribution for fluid can be expressed as

$$f_i(\mathbf{x} + \mathbf{e}_i\Delta x, t + \Delta t) - f_i(\mathbf{x}, t) = -\frac{f_i(\mathbf{x}, t) - f_{i,\mathrm{eq}}(\mathbf{x}, t)}{\tau_f} \tag{10}$$

where $f_{i,\mathrm{eq}}(\mathbf{x}, t)$ is the equilibrium distribution, which is defined by

$$f_{i,\mathrm{eq}} = \omega_i \rho_f \left(1 + 3\mathbf{e}_i \cdot \mathbf{u} + \frac{9}{2}(\mathbf{e}_i \cdot \mathbf{u})^2 - \frac{3}{2}\mathbf{u}_i \cdot \mathbf{u}\right) \tag{11}$$

The density and velocity of the fluid can be calculated by

$$\rho_f = \sum_i f_i \tag{12}$$

$$\rho\mathbf{u} = \sum_i \mathbf{e}_i \cdot f_i \tag{13}$$

In the simulation, the dimensionless kinematic viscosity υ and the dimensionless diffusivity for oxygen in LBE are given by

$$\upsilon = \frac{1}{3}\left(\tau_f - \frac{1}{2}\right)\Delta x \tag{14}$$

$$D = \frac{1}{3}\left(\tau - \frac{1}{2}\right)\Delta x \tag{15}$$

Then the Schmidt number is determined as

$$Sc = \upsilon/D = (2\tau_f - 1)/(2\tau - 1) \tag{16}$$

In the simulation, non-slip boundary conditions are applied on the walls of the rectangular container, while free surface condition is assumed at the interface of the cover gases. The flux of oxygen concentration on the wall is taken as zero. For the no-slip condition for the velocity at walls, it is implemented with the common bounce-back technique [14]. For the other boundary conditions for mass transport, we utilize an approach similar to the similar LBM model proposed by Inamuro et al. [12]. In this approach, the unknown distribution function on the wall are assumed to be the equilibrium distribution function given by Eq. (8) with a parameter C' and can be written as follows:

$$g_i = \omega_i C'(1 + 3\mathbf{e}_i \cdot \mathbf{u}_{\mathrm{wall}}) \tag{17}$$

where u_{wall} is the velocity vector at the boundary. The unknown parameter C' is determined based the fact that the

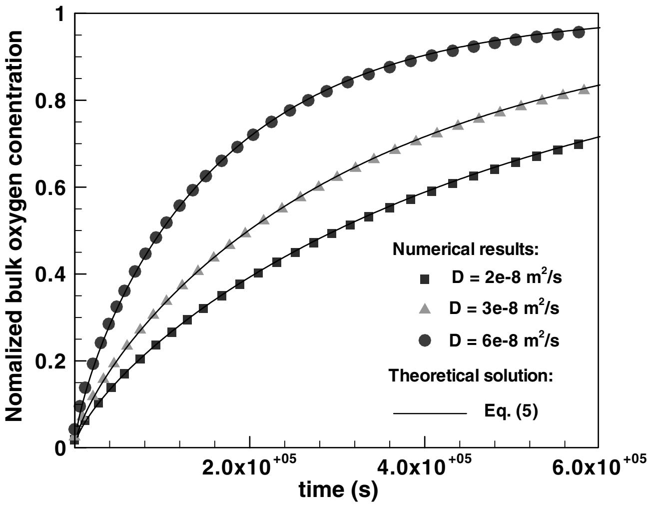

Fig. 2. Results comparison for pure diffusion in liquid LBE.

concentration of oxygen is equal to a given value of C_0. Substituting the above equation and the known distribution equation to Eq. (8), the parameter C' can be obtained

$$C' = \frac{(C_0 - \sum_i g_i)}{\sum_i \omega_i (1 + 3\mathbf{e}_i \cdot \mathbf{u}_{\text{wall}})} \tag{18}$$

where g_i denotes the known distribution function.

The benchmark study between the theoretical and numerical solutions on mass transfer for a rigid plane of stagnant liquid metal and the constant oxygen concentration on the surface has been made to valid lattice Boltzmann code. Fig. 2 shows the results comparison for pure diffusion in liquid LBE. As seen in Fig. 2, the numerical curves have very good agreement with that of theoretical solutions. To ensure lattice and time-step independence of the results, lattice size with 336 × 84, 408 × 102, and 528 × 132 were repeated respectively, with dimensionless time steps $\Delta t = 10^{-3}$ and 10^{-4}. No significant changes were found. Therefore, the results presented here are referred to 336 × 84 lattice size with dimensionless time step of 10^{-3}.

4. Results and discussion

Before the LBM simulation, we need identify the parameter applied in this work. In this work, the operating temperature for the LBE liquid flow is 500 °C. The density and dynamic viscosity are 1.012×10^4 kg/m^3 and 1.376×10^{-3} kg/m s, respectively [6]. The Schmidt number for oxygen transport ($Sc = 5$) are taken, corresponding to oxygen diffusion coefficient, $D = 2.72 \times 10^{-8}$ m^2/s. Three Reynolds numbers ($Re = 857$, 1143, and 1429) are tested to check the inlet velocity on the oxygen transport.

4.1. Flow pattern

Since the oxygen diffusion time is much longer than the developing of velocity, the unsteady terms for the momentum transport are neglected. The steady-state velocity distributions are demonstrated in Fig. 3 for three different inlet–outlet location at $Re = 1143$. Similar patterns are shown at higher Re. As seen in Fig. 3, the location of inlet and outlet changes the convection flow obviously. For the case A, the LBE flow is injected near the bottom wall and passes through the container at the outlet near the top wall. One counterclockwise rotating flow cell is generated in the left-top corner region. From the velocity vector plots of case B, we can see that there are one counterclockwise rotating flow cells in the left-top corner region while a clockwise rotating flow cell occurs at the right-bottom corner. For the case C, the LBE fluid flows along the free surface and then passes through the container at the outlet near the bottom wall. One clockwise rotating flow cell forms at the right-bottom corner. Since oxygen concentration at the free surface is much larger than that inside the container, it is expected that these circulated flow cells can mix the oxygen quickly and then enhance the oxygen transport.

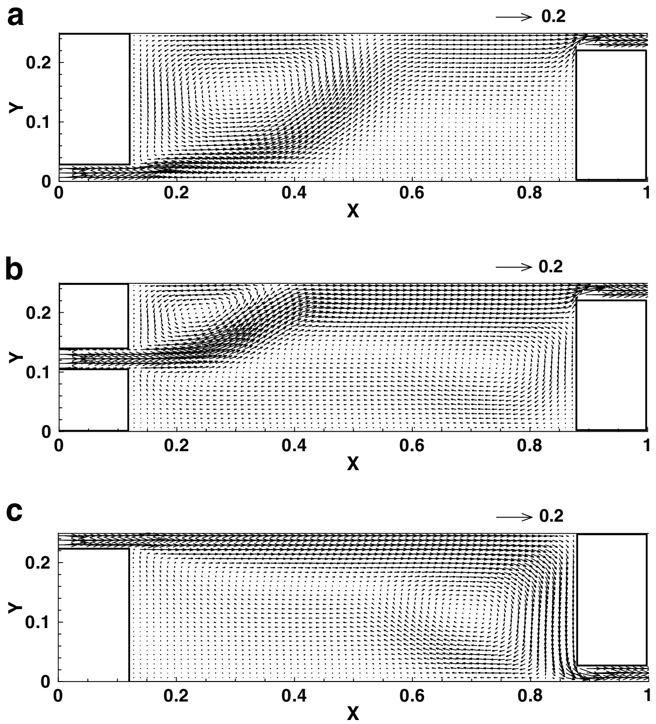

Fig. 3. Flow pattern under different forced convection mode ($Re = 1143$): (a) case A, (b) case B and (c) case C.

4.2. Oxygen transport

Once the oxygen controlled technique is applied to mitigate corrosion, one important task is to find a way to mix oxygen in a low concentration uniformly and quickly. In this section, our emphasis places on the forced convection on the oxygen transport and the consumption of the oxygen on the wall is neglected. To render the oxygen concentration dimensionless, the oxygen concentration is normalized by the dissolving oxygen concentration at the liquid surface.

Fig. 4 shows the oxygen concentration contours at different times ($t = 40$, 150, 350 and 1000 s) for different case at $Re = 1143$ and $Sc = 5$ (corresponding to the values of ρ and μ for liquid lead in Table 1 and oxygen diffusion coefficient $D = 2.72 \times 10^{-8}$ m^2/s). The concentration contours at $t \geqslant 350$ s for each case are similar to their velocity distributions shown in Fig. 4. This clearly shows that force convection is the dominant driving force for oxygen transfer. From all the figures, witness that flow cell can enhance the oxygen transport evidently. At $t = 40$ s, it is noted that oxygen firstly spreads along the left side wall of the container from the free surface for the case A due to the counterclockwise rotation flow cell. As time increases, oxygen continues o transfer from the upper part to the lower part and fills entire region of the container gradually. Under case B, the oxygen transport in the right bottom corner is much faster since the clockwise rotation cell occurs. Similar phenomena also can be found in the case C.

To test and calibrate oxygen sensors, the oxygen sensors will be placed at three columns inside the container ($X = 0.25L$, $0.5L$, and $0.75L$). The oxygen concentration at oxygen sensor locations at different time is illustrated in Fig. 5 for different Sc numbers at $Re = 1143$ and $Sc = 5$ for different cases. As found in the figures, the oxygen concentration in different location increases as time increases. For all the cases, the variation of oxygen concentration with time is different with locations. Since the convection is the dominant force for oxygen transport, all of the phenomena can be well explained by checking the flow pattern. From all of the curves, it is noticed that the variation of oxygen concentration in the location near the upper free surface is smaller comparing that far away the

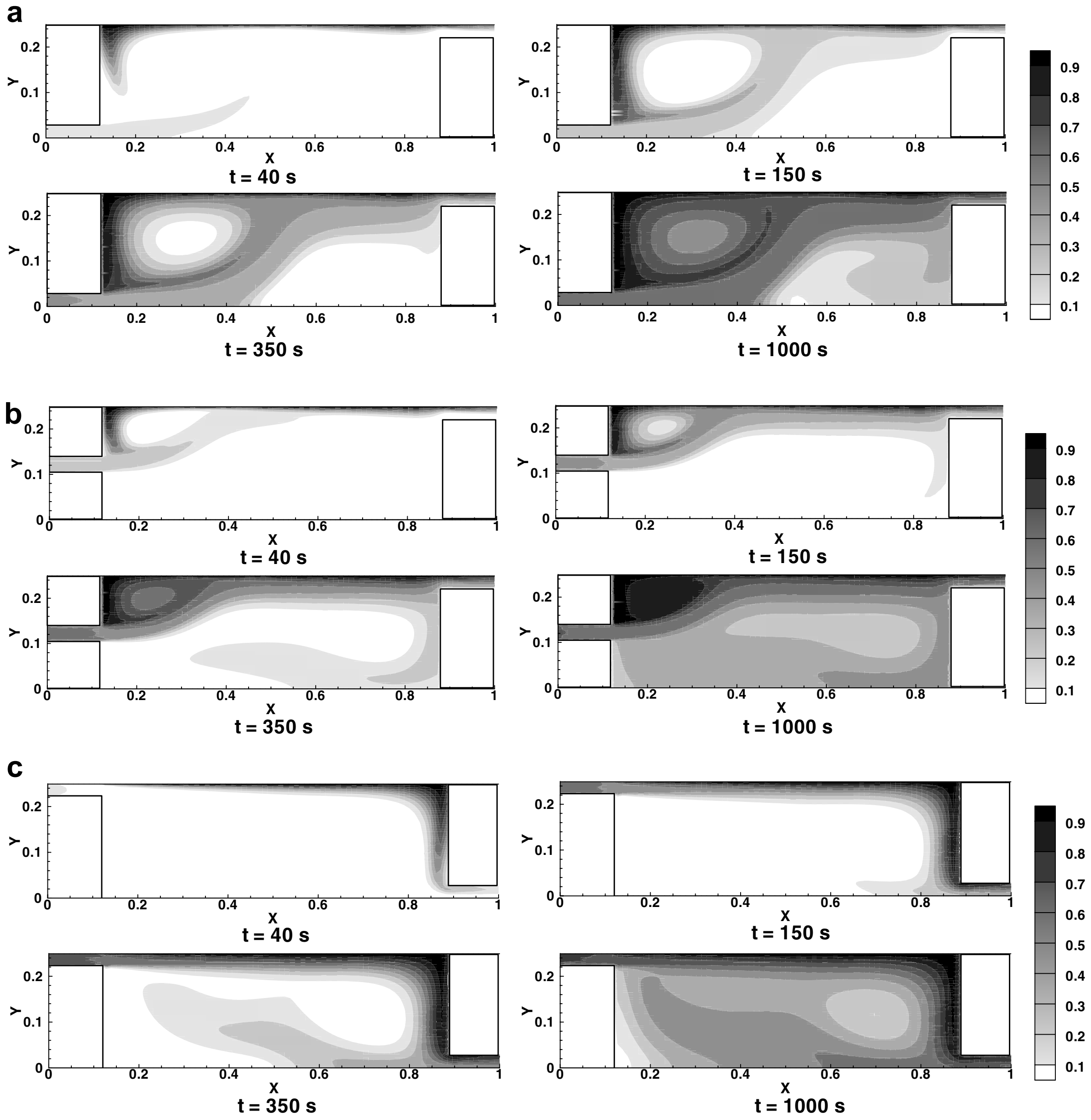

Fig. 4. Oxygen concentration contours at different times ($t = 40$, 150, 350 and 1000 s) for different convection mode. $Re = 1143$ and $Sc = 5$ for all cases: (a) case A, (b) case B and (c) case C.

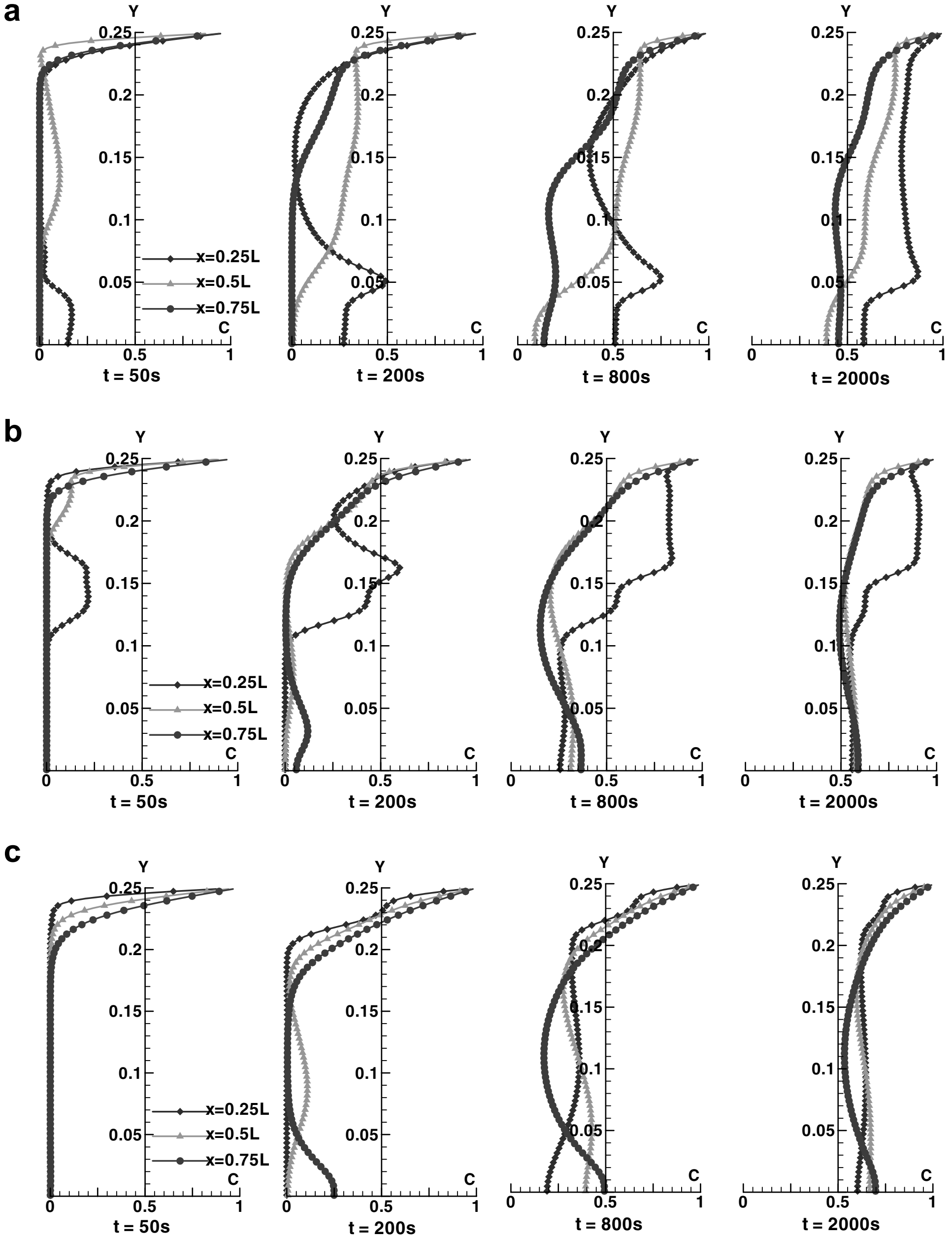

Fig. 5. Oxygen concentration at oxygen sensor locations at different time. $Re = 1143$ and $Sc = 5$ for all cases: (a) case A, (b) case B and (c) case C.

free surface since the mixture of hydrogen and water steam covers the upper free surface and the oxygen transport in this region is faster and easy to get the equilibrium. Hence, it is better to locate the oxygen sensor a certain distance away from the free surface to get good performance. For the case A, since the counterclockwise rotation flow cell at the left-top corner is closer to the interface, the oxygen concentration transportation here is much faster than that in the other region. Similar situation also can be found in the case B. From the figures, it can be found that the oxygen transport at the case C is more uniform comparing the other cases.

One of critical parameter to evaluate the performance of forced convection is the oxygen transfer speed. Once the oxygen transport speed is slow, the oxide layer near the wall can not form and the steel wall will dissolved directly. Hence, severe corrosion will occur. To check the oxygen transfer speed, we examined the bulk concentration under different forced convection conditions and different Reynolds number, as shown in Fig. 6. For all the case, the bulk oxygen concentration will increase with increasing of time. At the initial period, the bulk oxygen concentration will increase sharply and the effect of convection on oxygen transfer is more intensive. Of these three different forced convection modes, case C seems to be the faster way to get equilibrium for oxygen transfer comparing the other cases although bulk oxygen concentration for case A in the initial stage is faster. Fig. 6 also indicates the nature

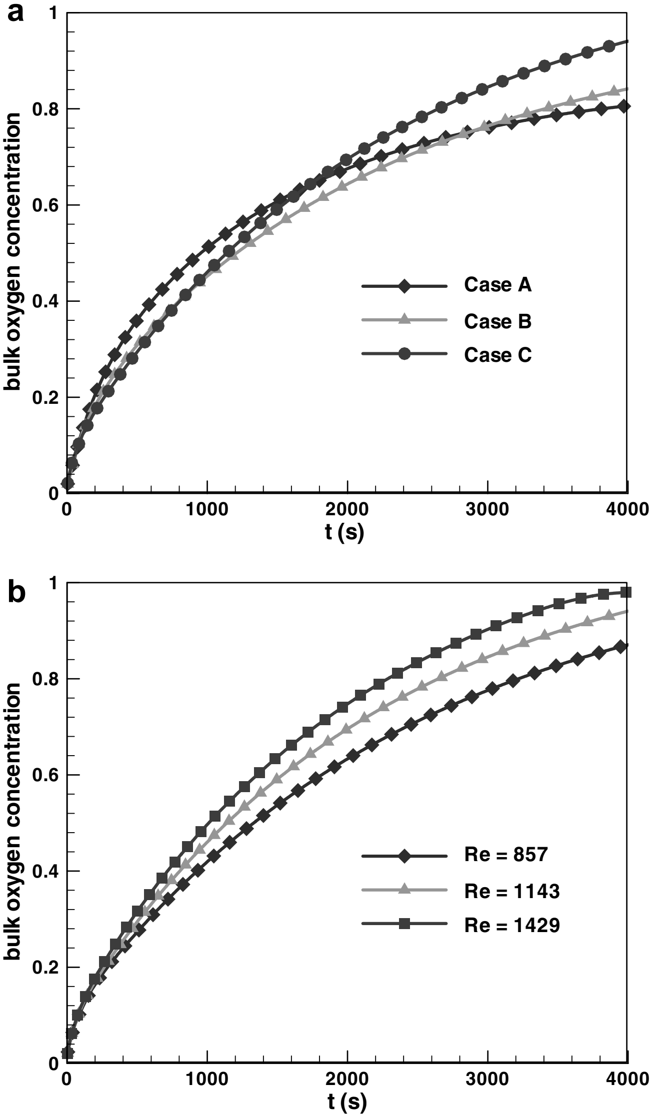

Fig. 6. The bulk oxygen concentration in the liquid as a function of time for different boundary conditions. $Sc = 5$ for all cases. (a) $Re = 1143$ and (b) case C.

convection can enhance the oxygen transfer evidently. It takes about $\sim 10^4$ s for the oxygen concentration to reach the ~90% of the input concentration from the top for case C at $Re = 1143$ and $Sc = 5$ while the pure diffusion would takes $\sim 10^6$ s. The effect of inlet flow velocity on oxygen transfer speed is illustrated in Fig. 5(b). Notes that the larger the Reynolds number is, the faster the oxygen transport will be.

Fig. 7 shows the average Sherwood number at the interface of cover gas and liquid metal as a function of time for different boundary conditions. Here the Sherwood number is defined by

$$Sh = \frac{KL}{D} = \frac{1}{1 - C_{\text{bulk}}} \frac{\partial C}{\partial Y}\bigg|_{\text{Free surface}} \tag{19}$$

where K is the mass transfer coefficient (m/s). For all cases, the average Sherwood numbers drop significantly with time

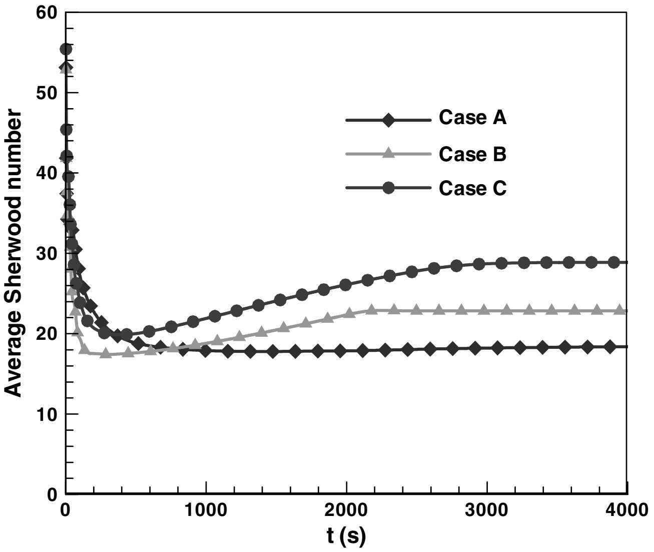

Fig. 7. The average Sherwood number at the interface of cover gas and liquid metal as a function of time for different boundary conditions. $Re = 1143$ and $Sc = 5$ for all cases.

at first 200 s. After that, the average Sherwood number almost keeps constant for case A. However, for case B and case C, the average Sherwood number increase slightly as time increases and keep constant after approximate 2000 s. From the figure, it also can be found that the Sherwood number in case C is larger than that in the other case after the initial stage. Considering that the larger Sherwood number corresponds to the stronger mass transfer at the interface is, more oxygen is transported into the liquid in case C comparing the other cases.

5. Conclusion

Corrosion of contaminant and structural materials presents critical challenges in the use of lead alloys. Active oxygen control is a key method to mitigate corrosion by forming a protective oxide layer. In this paper, the oxygen control system with cover gas scheme is investigated. To mix the oxygen in the LBE system uniformly and quickly, the forced convection is being proposed to enhance the oxygen transport.

In this paper, three kinds of different force convection mode for our experimental setup of containers in nuclear engineering applications are considered. The lattice Boltzmann simulations of the forced convection driven oxygen transfer in the liquid lead and LBE are presented in detailed. The simulation results show that the force convections induced by all the boundary conditions greatly enhance the oxygen transport in the liquid metal of our system. The most efficient one is under boundary condition C, in which the injection inlet of liquid LBE locates at the top of the container. It takes about $\sim 10^3$ s for the oxygen concentration in the whole field to reach ~90% of the input concentration from the top at $Re = 1143$ and $Sc = 5$ while the pure diffusion would take $\sim 10^6$ s.

Acknowledgements

The authors would like to thank the financial support from DOE TRP program.

References

[1] B.F. Gromov, Y.I. Orlov, P.N. Martynov, V.A. Gulevsky, The problems of technology of the heavy liquid metal coolants (lead–bismuth, lead), in: Proceeding of Heavy Liquid Metal Coolants in Nuclear Technology (HLMC-98), vol. 1, Obninsk, 1998, pp. 87–91.

[2] P.N. Martynov, Y.I. Orlov, Slagging processes in lead–bismuth: prevention and elimination of critical situations, in: Proceeding of Heavy Liquid Metal Coolants in Nuclear Technology (HLMC-98), vol. 2, Obninsk, 1998, pp. 565–576.

[3] V.A. Gulevsky, P.N. Martynov, Y.I. Orlov, M.E. Chemov, Application of hydrogen/water vapor mixtures in heavy coolant technology, in: Proceeding of Heavy Liquid Metal Coolants in Nuclear Technology (HLMC-98), vol. 2, Obninsk, 1998, pp. 668–677.

[4] N. Li, Active control of oxygen in molten lead–bismuth eutectic systems to prevent steel corrosion and coolant contamination, J. Nucl. Mater. 300 (2002) 73–81.

[5] G. Müller, A. Heinzel, G. Schumacher, A. Weisenburger, Control of oxygen concentration in liquid lead and lead–bismuth, J. Nucl. Mater. 321 (2003) 256–262.

[6] J. Zhang, N. Li, Review of studies on fundamental issues in LBE corrosion, Los Alamos National Laboratory Report, LA-UR-04-0869, 2004.

[7] C.H. Lefhalm, J.U. Knebel, K.J. Mack, Kinetics of gas phase oxygen control system (OCS) for stagnant and flowing Pb–Bi systems, J. Nucl. Mater. 296 (2001) 301–330.

[8] N. Li, Active control of oxygen in molten lead–bismuth eutectic systems to prevent steel corrosion and coolant contamination, J. Nucl. Mater. 300 (2002) 73–81.

[9] T.W. Darling, N. Li, Oxygen concentration in liquid Pb–Bi eutectic, Los Alamos National Laboratory Technical Report, LA-UR-02-3036, 2002.

[10] D. H Rothman, J.M. Keller, Immiscible cellular-automaton fluids, J. Stat. Phys. 52 (1988) 1119–1127.

[11] R. Holme, D.H. Rothman, Lattice-gas and lattice-Boltzmann models of miscible fluids, J. Stat. Phys. 68 (1992) 409–429.

[12] T. Inamuro, M. Yoshino, H. Inoue, R. Mizuno, F. Ogino, A lattice Boltzmann method for a binary miscible fluid mixture and its application to a heat-transfer problem, J. Comput. Phys. 179 (2002) 201–215.

[13] X. Shan, G. Doolen, Multicomponent lattice-Boltzmann model with interparticle interaction, J. Stat. Phys. 81 (1995) 379–397.

[14] O. Filippova, S. Succi, F. Mazzocco, C. Arrighetti, G. Bella, D. Hänel, Multiscale lattice Boltzmann schemes with turbulence modeling, J. Comput. Phys. 170 (2001) 812–829.

[15] H. Yu, S. Girimaji, Li. Luo, DNS and LES of decaying isotropic turbulence with and without frame rotation using lattice Boltzmann method, J. Comput. Phys. 209 (2005) 599–616.

[16] M. Yoshino, T. Inamuro, Lattice Boltzmann simulations for flow and heat mass transfer problems in a three-dimensional porous structure, Int. J. Numer. Methods Fluids. 43 (2003) 183–198.